

NICI Technical Memorandum

Memo Number: 01:03

Date: August 31, 2001

Subject: NICI Optical Surface Requirements

Distribution: Dtoomey, Cftaclas

1. Introduction.

The wave front entering NICI results from the interaction of the atmosphere, telescope optics, telescope alignment and any low order corrections applied to the primary. The coronagraph and AO system alter this wave front in a positive way but the many optical elements within the instrument can degrade the wave front. We can derive surface figure requirements for the NICI optical elements by limiting the impact of any negative consequences. The instrument wave front sensor (WFS) is critical to NICI's performance but it has no way of discerning whether the phase errors it measures arise in the sensor, the instrument or the atmosphere. Consequently, figure errors in the sensor must be contained in order to prevent large bias corrections. We also want to that the images generated within the WFS are high enough quality to not impede operation of the sensor. In general, this requires that the sensor remain in its linear range and this is related to the bias concerns above.

In the science channel, there are two main areas of concern: image Strehl and scattered light. Maintaining a high Strehl is necessary to assure that NICI produces a quality image, and controlling scattered light is necessary to assure that atmospheric and telescope scatter limit instrument residual background rather than instrumentally induced scatter. At this time, we cannot know exactly the properties of the wave front entering the instrument but we can require that for "best-case" assumptions, any negative alterations of the wave front introduced by NICI are minimal. To this end, we assume that the telescope is perfect and does not contribute to the instrument wave front. We also assume atmospheric conditions are optimal so residual atmospheric scatter is at a minimum. This leads to the tightest surface scatter requirements.

2. NICI Camera Optical Elements

In Table 1 we list all the NICI optical elements in the science beam. For this discussion, we divide the instrument into two major optical subassemblies: the wave front sensor relay (warm) and the Cryo-optical camera (cold). Technically, the front of the dewar window is the interface between these two but functionally the occulting mask is a more appropriate boundary. The WFS relay images the telescope focus to the first instrument focus (occulting mask) and the cryo-optics image the first focus to the second or detector focus so the occulting mask is the functional boundary between these two re-imaging systems. For each of the named elements in Table 1 we give the following information:

- a. Surface-to-wave front conversion factor. This gives the multiplier for converting from a surface rms measured at normal incidence to a wavefront rms as measured in the instrument. For a mirror at normal incidence, this is a factor of 2 and for a transmissive element it is $\sqrt{2}(n-1)$ where n is the index of refraction of the lens element. Assuming a glass like Calcium Fluoride ($n=1.43$) for the dewar window this factor is 0.61. There is also a possible perspective improvement in the figure given by the cosine of the angle of incidence. This is included for elements like fold-flats with significant tilt with respect to the beam.
- b. Correction factor. This gives any wave front improvement factor associated with that element. Wave front improvement is applicable to elements that come before the wave front sensor pickoff and have their figure error sensed and corrected to some level. Determination of this factor is discussed below.
- c. Strehl weight. This is just a measure of whether or not errors at this surface contribute to Strehl loss. It is unity for most elements but elements at or near a focal plane (mask and dewar window) cannot add phase error to the pupil since they are simply re-imaged at the final focus.
- d. Scatter weight. This is a measure of whether or not the element contributes to the stellar scatter halo. It is unity for all elements illuminated by the image core of the occulted star and 0 otherwise.
- e. Difficulty. This is a rough assessment of the difficulty in making a given component and allows for apportioning wave front error to minimize cost. Aspheric elements get a factor of 1.2 and flat elements a factor of 0.8. Warm aspheric elements are given unit difficulty as described in Section 6.
- f. Strehl Multiplier. This is the product of items a, b, c and e.
- g. Scatter Multiplier. This is the product items a, d and e.

There could be a small asymmetry between the Strehl in the two NICI imaging channels because, if a dichroic is used, one channel is reflected and the other transmitted. We have taken the worst case of the beam reflected at 45° .

3. The Adaptive Optics Correction Factor

The adaptive optics system filters the wave front power spectrum. One could model this filter as perfect up to its Nyquist frequency but this is grossly optimistic since the ability of a given DM to correct errors degrades long before the Nyquist limit. Instead of such an idealized model we can use a more heuristic approach and think of the AO system as a square wave filter $F(f, f^*)$ having an “effective” cutoff spatial frequency f^* below which it is perfect and above which it is totally ineffective. To estimate f^* we can note that if σ_i is the wave front rms going in to the AO system and σ_o is the wave front rms after the AO system then for any power law power spectrum we have $\sigma_o = (f^*)^{1-\gamma/2} \sigma_i$, where γ is the spectral index of the power law. Wave fronts that simulate the effects of NICI’s 85-element system (supplied by M. Northcott) give $f^* = 3.55$ for the effective cutoff of the system. For the spectrum of optical figure errors

γ is closer to 3, so using the value of f^* derived above and $\gamma = 3$ we get $\frac{\sigma_o}{\sigma_i} = 0.53$ for

the wave front correction factor reported in Table 1. Note that for a circular array of 85 equally spaced actuators one would have predicted $f^* = 5$ grossly overestimating the capabilities of the AO system and overestimating the residual Strehl by about 30%.

4. Strehl Ratio and Scattered Light

Strehl depends on total wave front error regardless of spatial frequency domain. Strehl considerations apply to images of sources not suppressed by the coronagraph so all elements are illuminated by the beam. The difficulty of making a given optic is determined by its normal incidence surface requirement not by its effective contribution to the instrument wave front. We assume that each element has a surface figure error of $\sigma_e = \sigma_c d_e$ where d_e is the difficulty of making that element, and σ_c is a constant. Thus if all elements are equally difficult to make they would all have the same surface requirement no matter what their contribution to the beam. This creates an equitable distribution of the cost of the optics independent of how they are oriented in the instrument. The contribution of this element to the instrument wave front error is then:

$$w_e = \sigma_e SW_e C_e W_e = \sigma d_e SW_e C_e W_e = \alpha_e \sigma$$

where SW is the surface to wave front conversion factor, C is the wave front correction factor, W is the Strehl weight and α is the Strehl multiplier. For a given wave front requirement σ_o we have:

$$\sigma_o = \sqrt{\sum_i \alpha_i^2 \sigma_c^2} = \sigma_c \sqrt{\sum_i \alpha_i^2}.$$

This permits determination of the constant σ_c and the surface requirement for each optic from $\sigma_i = d_i \sigma_c$. A Strehl of 0.9 @ 2200nm gives a permissible instrument wave front error of 0.05 waves or 0.18 waves @ 633 nm. The rss of all Strehl multipliers is 4.47 (Table 1) giving an effective rms per element of 0.04 waves @ 633 nm. To get the permissible error for individual elements we multiply the per-element rms by the difficulty and Strehl weight for that element. This gives the surface errors in Column I of Table 1.

Scattered light considerations apply to bright sources that suppressed by the coronagraph. Only optical elements fully illuminated by the central object, i.e. every element ahead of the occulting mask, contribute to the scattered light halo. It remains to define a permissible level of scatter. Ignoring telescope errors, residual scatter will arise from atmospheric and instrument phase errors. Since these two effects are incoherent, the residual power spectrum will look like:

$$P(f) = \frac{\sigma^2}{2\pi D} k^{-3} + 0.000583 r_o^{-5/3} k^{-11/3}$$

The first term corresponds to spectrum of typical optical surfaces and the second is the Kolmogorov spectrum for the atmosphere. Here σ is the full aperture wave front error in waves and r_o is the Fried radius in meters. Because the spectrum of atmospheric turbulence is steeper than that of optical elements, at some field angle optical surface scatter will dominate over atmospheric scatter no matter how good the surface is. Thus, we have King's early observation that for a variety of telescopes, the point-spread functions of bright stars are all quadratic far from the star. The quadratic slope is characteristic of scatter from micro-roughness.

In the present case, we are interested in small angle scatter and we require that atmospheric scatter dominates over the NICI field. Equating these two terms in the equation above and recalling that the field angle is related to the spatial frequency by the grating equation, $\theta = \lambda k$, we can solve for the necessary σ for a given field size and r_o . Requiring that the atmosphere dominate over a larger field or by a larger factor will tighten the figure requirements. For a very good atmosphere with Fried length of ~30 cm at 550 nm (1.583 meters at K) and a field angle of 10 arcsec we get a permissible surface error of $\sigma = \lambda/14$ at 0.633 microns (See analysis in Appendix A). Using the implied wave front of $\lambda/7$ and dividing by the rss of all scatter multipliers we get the permissible, per element rms. In analogy with the Strehl calculation, this value is multiplied by the difficulty and the scatter weight to arrive at the goal rms for each element given in Column L of Figure 1.

5. The Wave Front Sensor

The wave front entering the telescope is of order 0.25 waves under the best conditions. Once the AO system has integrated for a few cycles, the corrected wave front is ~0.08 waves at K . The WFS samples the corrected beam in visible light so it is working with a wave front of $0.08 * 2.2 / .6 = 0.3$ waves (visible). Since the WFS optics are non-common path, it would be good practice if the wave front errors added by the WFS optics were less than the error we are trying to measure. The main reason for this is that the WFS is a null device. It detects the difference between two defocused images. Although figure errors anywhere in the telescope or sensor can be biased out of, or into the deformable mirror, the WFS will then no longer be working around zero and its operation is compromised.

Figure 1 is a schematic of the NICI wave front sensor. As with the camera itself the wave front sensor has two functional subassemblies: the relay between the telescope focus and the membrane mirror, and the camera between the membrane mirror and the lenslet array. The function of the relay is to take the telescope's $f/16$ beam and relay it to the membrane mirror at $f/60$. The camera images the two defocused focal plane images onto the lenslet array. The membrane mirror is the boundary between these two

functional units but can be part of either one. The membrane mirror oscillates between positive and negative curvature states to create defocused focal plane images on the lenslet array. In Figure 1, we have added red lines to indicate schematically the locations of these defocused images. Since the camera relays one or the other of these image planes onto the lenslet array one can see that for one of these images the membrane mirror is part of the relay and for the other it is part of the camera.

The defocused WFS images reflect all pupil phase errors in the beam regard of their origin. We want this total phase error to be to be less than the phase we are trying to measure, say one half, or 0.15 waves (visible). In very good conditions this only

increases the increases the sensed wave front by 12% $\left(\sqrt{1^2 + \left(\frac{1}{2}\right)^2} = 1.12 \right)$. The

membrane mirror itself is at a focus so we use only a very small part of it and can ignore its phase contribution. The quality of the lenslet array need only be good enough to assure good coupling with the fiber and will be addressed when the APD's and fibers are specified. Table 2 shows the WFS elements broken down as in Table 1., except in this case the concern is only the phase error added by each element. As in Table 1, we specify phase weight and relative manufacturing difficulty for each element. All elements are all either spheres or flats and we have assigned a uniform difficulty to them

As in the instrument analysis of the previous section, we calculate the rss of the phase multipliers and divide it into the goal wave front error to get a per element surface rms which is then multiplied by the difficulty to get the goal error for each component listed in Column F. For each element we can then calculate the effective rms and hence the effective Strehl (Column H) and the total for the WFS. It is clear that with so many elements and working at a short wavelength it is difficult to maintain a high Strehl. Fortunately, we are not making measurements at the focal plane but at the defocused image plane and the lenslet array will only be sensitive to the phase error over the small region it is imaging.

6. Optical Surface Requirements for NICI Elements

Comparing Columns I and L in Table 1 it can be seen that the figure requirements for the first four optical elements in NICI are driven more from scatter considerations than they are by Strehl considerations. Since we must meet the scatter requirements anyway, we will adopt the scatter values. Using these more stringent values, it is possible to recalculate the surface errors for the remaining optics but this produces no significant reductions in the tolerance.

The surface figure errors in Table 1 assume testing at 633 nm and normal incidence. They apply over any sub-aperture on the optic equal to the footprint of the beam. This is overly pessimistic since most of the warm elements are wave front corrected by the AO system and can be somewhat worse at low spatial frequencies. Recall that in the wave front sensor channel we required that the optics contributed no

more than one half of the wave front we are trying to measure because figure errors in the WFS are non-common path. In the warm relay optics, errors are common path so we can use the more relaxed requirement that figure errors within the AO correction bandwidth contribute less than one third of the *uncorrected* wave front. Thus, on average, the stroke

of the DM increases by about 5% $\left(\sqrt{1^2 + \left(\frac{1}{3}\right)^2} = 1.05 \right)$ due to errors on the optics. Since

we are correcting about one quarter wave @ 2.2 microns, it is about one wave in the visible and we are allowed $\lambda/3$ @ 0.633 microns as the effective rms error in this channel. According to Column M of Table 1, the calculated combined error in these elements is of order $\lambda/7$ (0.14 waves @ 0.633) so we can relax this specification by about a factor of two as long as we maintain the proper scatter specification outside the AO correction range. Because the two aspheric elements in this channel have relaxed low order figure requirements we have given them a unit difficulty factor.

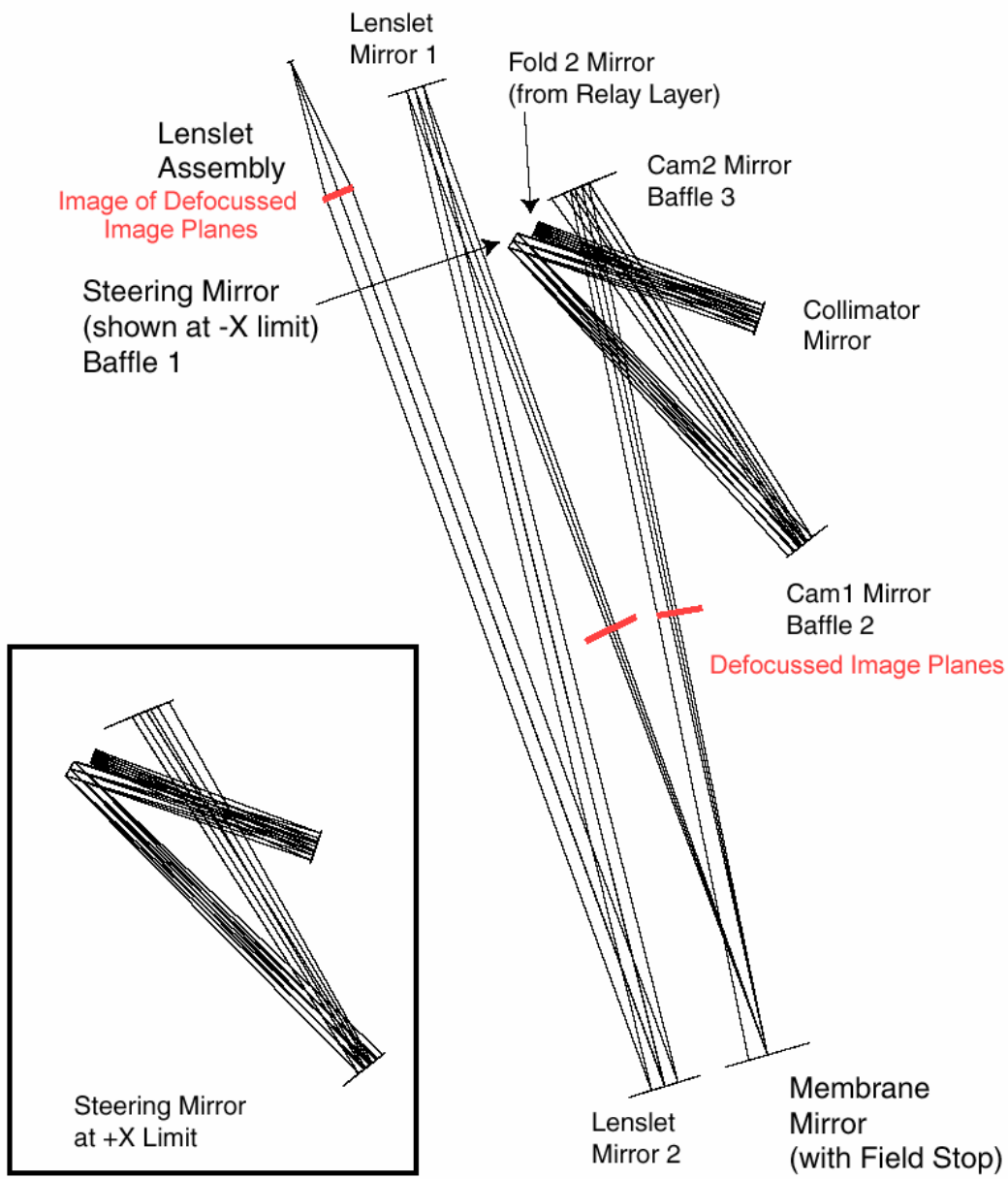
Table 3 reproduces the rms results from Tables 1 and 2 for each element. We also give the resulting wave front error in waves @ 633 nm and the inverse of the wave front error (i.e. the x in λ/x). We have added to Table 3 nominal values for the occulting mask substrate and dewar window in the science channel and for the membrane mirror and lenslet array in the WFS channel. Using the argument of the paragraph above, we have doubled the allowed RMS for the warm science optics (Column E) and treated this as a full aperture requirement. For these elements, however, we must be sure that we meet the scatter requirement.

The AO correction factor is 0.53 so, after the AO system, about half the input rms (numerically) remains in the beam. This is equivalent to saying that the figure measured over any sub-aperture of order one quarter the diameter of the full aperture should be half of the un-relaxed figure requirement (Column D of Table 3). We give this value in Column G of Table 3 as a sub-aperture requirement. In order to bridge the gap between the relaxed full aperture and constrained sub-aperture requirements we have added an intermediate specification over any sub-aperture that is one half the diameter of the beam footprint by using an averaging process. We can predict this specification by extrapolating from the constrained quarter aperture requirement or by interpolating from the relaxed full aperture requirement. We calculate both estimates and give their average in Column F of Table 3 as an intermediate specification. Sub-aperture specifications for the remaining elements in Table 3 come from the full aperture requirements in Column assuming a cubic power spectrum and the equations given in the discussion of the adaptive optics correction factor (Section 3). We can apply no significant relaxation of figure requirements for optical elements in the dewar without running the AO system in a biased state.

7. Surface Roughness.

Fine scale errors on optical surfaces produce a wide-angle scattering halo that can affect NICI in the form of an enhanced stray light background. It is desirable to limit this effect but since NICI is not a wide-field instrument, it makes no sense to drive the cost of

optics with a surface roughness requirement. We know that a basic requirement that would not represent a challenge to manufacturers is about 3 nanometers rms surface error. Using the surface-to-wave front conversions in Column C of Table 1 we can get the equivalent wave front for the NICI science channel as 5.43 times the single surface value. This predicts a Strehl loss due to micro-roughness of only 0.2% for the NICI science channel. For the wave front sensor channel, we take the surface conversions from Column B of Table 2 and add in the common path surfaces from the science channel. This gives an effective surface to wave front of 6.42 and a corresponding Strehl loss at 633 nanometers of order 3.6%. This is an overestimate since visible light scattered in the science channel is of no consequence. Consideration of only the optics in the WFS channel gives 2.5%. We conclude that a modest surface micro-roughness requirement of order 3 nanometers is acceptable for the NICI optics. We have assumed that this roughness is in the form of random surface errors rather than say parallel tooling marks from fine grinding or diamond turning. Such features can cause most of the scattered light to appear at a single diffracted order and give rise to scattered light problems.



200 mm

Gemini AO Coronagraph
WFS Layer
12 December, 2000 JCS

A	B	C	D	E	F	G	H	I	J	K	L	M
Element Name	Surface to Wavefront	Correction Factor	Strehl Weight	Scatter Weight	Difficulty	Strehl Multiplier	Surface RMS by Strehl @ 633nm	Effective RMS I ² D ² C	Scatter Multiplier	Surface RMS by Scatter	Effective RMS L ² C ² D	
1	Collimator	2.00	0.53	1.00	1.00	1.00	1.060	0.041	0.043	2.000	0.038	0.040
2	Deformable mirror	2.00	0.53	1.00	1.00	1.00	1.060	0.040	0.043	2.000	0.038	0.040
3	Camera mirror	2.00	0.53	1.00	1.00	1.00	1.060	0.040	0.043	2.000	0.038	0.040
4	Dichroic	1.41	0.53	1.00	1.00	1.00	0.747	0.040	0.030	1.410	0.038	0.029
5	Occulting Mask	0.71	1.00	0.00	0.00	1.00	0.000	0.000	0.000	0.000	0.000	0.000
6	Dewar Window	0.71	1.00	0.00	0.00	1.00	0.000	0.000	0.000	0.000	0.000	0.000
7	OAP 1	2.00	1.00	1.00	0.00	1.20	2.400	0.048	0.097	0.000	0.000	0.000
8	Fold Flat	1.41	1.00	1.00	0.00	0.80	1.128	0.032	0.045	0.000	0.000	0.000
9	Dichroic	1.41	1.00	1.00	0.00	0.80	1.128	0.032	0.045	0.000	0.000	0.000
10	Filter	0.71	1.00	1.00	0.00	0.80	0.568	0.032	0.023	0.000	0.000	0.000
11	Fold Flat 2	1.41	1.00	1.00	0.00	0.80	1.128	0.032	0.045	0.000	0.000	0.000
12	OAP 2	2.00	1.00	1.00	0.00	1.20	2.400	0.048	0.097	0.000	0.000	0.000
13												
14												
15												
16							4.43		0.178	3.74		0.08
17							RMS Strehl Multiplier		total RMS @0.6 (wave front)	RMS Scatter multiplier		total RMS@0.6 (wavefront)
18												

Table 1. Surface Figure Error Budget for NICI science channel

	A	B	C	D	E	F	G	H
1	Element Name	Surface to Wavefront	Phase Weight	Difficulty Multiplier	Phase Multiplier	Surface RMS (Waves)	Effective RMS (F*C*B)	Component
2								Strehl Factor
3	Dichroic (Back Surface)	0.355	1	1	0.355	0.038	0.0134	0.993
4	Collimator Mirror	2	1	1	2	0.038	0.0753	0.799
5	Steering Mirror	2	1	1	2	0.038	0.0753	0.799
6	Cam1 Mirror	2	1	1	2	0.038	0.0753	0.799
7	Cam2 Mirror	2	1	1	2	0.038	0.0753	0.799
8	Membrane Mirror	2	0	1	0	0.000	0.0000	1.000
9	Lenslet Mirror 1	2	1	1	2	0.038	0.0753	0.799
10	Lenslet Mirror 2	2	1	1	2	0.038	0.0753	0.799
11	Lenslet Array	0.5	0	1	0	0.000	0.0000	1.000
12								
13					4.912		0.151	0.259
14					RSS of		Wavefront	Total
15					Phase		RMS of Phase	WFS Strehl
16					Factors		Surfaces	

Table 2. Surface Figure Error Budget for NICI WFS channel

	A	B	C	D	E	F	G
1	NICI Science Channel						
2						1/Wavefront	
3				From	Over Beam	Over Half	Over Quarter
4	Element Name	Surface RMS	Wavefront RMS	Table 1	Footprint	Beam Footprint	Beam Footprint
5		(waves)	(waves)				
6	Collimator	0.038	0.076	13.2	6.6	13.956	26.3
7	Deformable mirror	0.038	0.076	13.2	6.6	13.956	26.3
8	Camera mirror	0.038	0.076	13.2	6.6	13.956	26.3
9	Dichroic	0.038	0.076	13.2	6.6	13.956	26.3
10	Occulting Mask	0.050	0.1	10.0	10.0	14.142	20.0
11	Dewar Window	0.050	0.1	10.0	10.0	14.142	20.0
12	OAP 1	0.048	0.096	10.4	10.4	14.731	20.8
13	Fold Flat	0.032	0.064	15.6	15.6	22.097	31.3
14	Dichroic (Front Surface)	0.032	0.064	15.6	15.6	22.097	31.3
15	Filter	0.032	0.064	15.6	15.6	22.097	31.3
16	Fold Flat 2	0.032	0.064	15.6	15.6	22.097	31.3
17	OAP 2	0.048	0.096	10.4	10.4	14.731	20.8
18							
19	NICI Wave Front Sensor						
20						1/Wavefront	
21	Element Name	Surface RMS	Wavefront RMS	1/Wavefront	Over Beam	Over Half	Over Quarter
22		(Waves)	(waves)		Footprint	Beam Footprint	Beam Footprint
23	Dichroic (Back Surface)	0.0380	0.076	13.2	13.2	18.6	26.3
24	Collimator Mirror	0.0380	0.076	13.2	13.2	18.6	26.3
25	Steering Mirror	0.0380	0.076	13.2	13.2	18.6	26.3
26	Cam1 Mirror	0.0380	0.076	13.2	13.2	18.6	26.3
27	Cam2 Mirror	0.0380	0.076	13.2	13.2	18.6	26.3
28	Membrane Mirror	0.0500	0.1	10.0	10.0	14.1	20.0
29	Lenslet Mirror 1	0.0380	0.076	13.2	13.2	18.6	26.3
30	Lenslet Mirror 2	0.0380	0.076	13.2	13.2	18.6	26.3
31	Lenslet Array	0.1000	0.2	5.0	5.0	7.1	10.0
32							
33	Note: All RMS values are waves @ 633 nm						

Table 3. Final wave front specification for NICI optical elements

Appendix A. Evaluation of Equality of Figure and Kolmogorov Power Spectra

$D := 8$ Telescope Aperture (meters)

$\lambda := 2.2$ Operating wavelength (microns)

$r_{ov} := 30$ Fried Radius @ 550 nanometers (cm)

$n := 3$ Spectral index of figure error PSD

$\sigma := .04$ RMS Figure error (waves)

$$r_{ok} := \frac{r_{ov}}{100} \cdot \left(\frac{\lambda}{.55} \right)^{\frac{6}{5}} \quad r_{ok} = 1.583 \quad \text{Fried radius at operating wavelength (meters)}$$

$$\theta_o := 0.206265 \cdot \frac{\lambda}{D} \quad \theta_o = 0.057 \quad \text{Diffraction radius (arcsec)}$$

$$\rho_{max} := \frac{10}{\theta_o} \quad \rho_{max} = 176.296 \quad \text{\# of Airy rings in 10 asec radius at K}$$

$$K(\rho) := .000583 \cdot \left(\frac{D}{r_{ok}} \right)^{\frac{5}{3}} \rho^{-\frac{11}{3}} \quad \text{Kolmogorov Spectrum (waves**2/cyc/arcsec**2)}$$

$$F(\rho) := \frac{n-2}{2 \cdot \pi} \sigma^2 \rho^{-n} \quad \text{Figure error PSD same units as K}$$

$$j := 1..175 \quad r_j := j \quad \theta_j := r_j \cdot \theta_o \quad \text{Scatter angle (arcsec)}$$

$$\text{Air}_j := K(r_j) \quad \text{Fig}_j := F(r_j)$$

Suppose the two spectra are equal at $\rho = \alpha$, then:

$$\sigma(\alpha) := \sqrt{K(\alpha) \cdot \frac{2 \cdot \pi}{n-2} \cdot \alpha^n} \quad s_j := \sigma(r_j) \quad \text{Figure req for intersection (waves wavefront @K).}$$

$$s_{vis_j} := s_j \cdot \frac{\lambda}{2 \cdot 0.633} \quad \text{Figure req for intersection (waves surface @HeNe).}$$

$$d := s_{vis_{175}} \quad d = 0.073 \quad \sigma_{vis} := \frac{1}{d} \quad \sigma_{vis} = 13.789$$

